Experimental Cell Research **261,** 199–208 (2000)
doi:10.1006/excr.2000.5052, available online at http://www.idealibrary.com on IDEAL®

Phosphorylation of NPA58, a Rat Nuclear Pore-Associated Protein, Correlates with Its Mitotic Distribution

Radhika Ganeshan and Veena K. Parnaik[1]

Centre for Cellular and Molecular Biology, Hyderabad 500 007, India

At the onset of mitosis in higher eukaryotic cells, the nuclear envelope and its components including subunits of the nuclear pore complexes are disassembled, and these are reassembled toward the end of mitosis. We have studied the role of protein phosphorylation in this process, by investigating the phosphorylation status of a specific pore-associated protein during mitosis. Using a monoclonal antibody, mAb E2, earlier shown to inhibit nuclear protein import in rat fibroblast cells, we have identified a 58-kDa protein termed NPA58 that is partially associated with nuclear pores based on a high degree of coincident immunofluorescence in dual labeling experiments with mAb 414, a well-studied pore-complex-reactive antibody. NPA58 is specifically phosphorylated during mitosis and dephosphorylated upon release from metaphase arrest. Confocal microscopy analysis shows that NPA58 is dispersed in the cytoplasm early in mitosis when it is phosphorylated, while its relocalization in the reforming nuclear envelope during telophase temporally correlates with its dephosphorylation upon release from metaphase arrest. Our data provide *in vivo* evidence that the modifications mediated by phosphorylation and dephosphorylation are required for regulating the mitotic localization of a nuclear-pore-associated protein.

Key Words: **nuclear pore complex; mitotic phosphorylation; nuclear assembly.**

INTRODUCTION

The nuclear envelope of eukaryotic cells consists of two lipid bilayers constituting the outer and inner nuclear membranes which are perforated by supramolecular aqueous channels called the nuclear pore complexes (NPCs) and a filamentous network termed the nuclear lamina that lines the nucleoplasmic face of the inner nuclear membrane [1–3]. The NPCs are evolutionarily conserved, elaborate structures that mediate signal-dependent, bidirectional nucleocytoplasmic transport by interacting with soluble transport factors [4–8]. The basic structural framework of the NPC is conserved from yeast to vertebrates and has been demonstrated by high-resolution electron microscopy to consist of a spoke–ring complex, a central transporter region, and attached cytoplasmic and nuclear filaments [9–11]. The NPCs in vertebrates have an estimated mass of 125×10^6 Da [12] with dimensions of 120×80 nm for the central framework. On its cytoplasmic face, the peripheral extensions of the NPC consist of ~50-nm filaments, which provide initial docking sites for nuclear import [13–15]. On the nucleoplasmic face, the NPC-attached nuclear filament bundles form a symmetric structure described as the nuclear basket [16] which can extend into the nuclear interior up to 350 nm. In certain cell types such as amphibian oocytes, the basket may also be attached to a nuclear lattice [14]. The NPCs are composed of multiple copies of polypeptides called the nucleoporins, all of which have been recently identified and localized in yeast nuclear pores [17]. The NPCs in vertebrates are larger and are believed to consist of several additional members. Many of the known nucleoporins contain FXFG, GLFG, and FG sequence motifs and are also modified by O-linked *N*-acetylglucosamine [18, 19].

In higher eukaryotes the nuclear envelope disassembles during mitosis in a process characterized by depolymerization of the nuclear lamina into soluble A-type and vesicle-associated B-type lamins, fragmentation of the nuclear membranes, breakdown of the NPCs, and dispersal of NPC proteins in the cytoplasm. These processes are initiated at prometaphase and are generally believed to be regulated by phosphorylation of the individual components of the nuclear envelope. Nuclear assembly has been studied extensively in cell-free systems for nuclear membrane vesicles and the lamins [20]. Disassembly of the nuclear lamina is regulated through phosphorylation by the cyclin-B-dependent $p34^{cdc2}$ kinase [21, 22] whereas reassembly is likely to involve dephosphorylation. Integral membrane proteins such as lamin-associated polypeptides, LAP1 and LAP2, and lamin B receptor (LBR) are also phosphor-

[1] To whom correspondence and reprint requests should be addressed at Centre for Cellular and Molecular Biology, Uppal Road, Hyderabad 500 007, India. Fax: +91-40-7171195. E-mail: veenap@ccmb.ap.nic.in.

0014-4827/00 $35.00

ylated during mitosis and this is believed to be significant for their dissociation from the lamina during nuclear envelope breakdown [23, 24]. Subsequently in mammalian somatic cells, integral membrane proteins are observed to be dispersed throughout the peripheral endoplasmic reticulum [25, 26]. Disassembly of NPCs is likely to proceed through the formation of subcomplexes that become dispersed in the cytoplasm [27]. Toward the end of mitosis, the constituents of the nuclear envelope are reassembled from the mitotic precursor pool in a stepwise manner.

Some insights into the role of phosphorylation during the mitotic breakdown and reassembly of NPCs have been gained from studies on individual pore proteins. Two nuclear pore glycoproteins, p200 and p97 have been shown to be specific targets for $p34^{cdc2}$ kinase in both *in vivo* and *in vitro* assays using *Xenopus* eggs [27]. In another study, the nuclear pore membrane glycoprotein gp210 was demonstrated to be phosphorylated in mammalian mitotic cells but not during interphase, and three other nucleoporins, Nup153, Nup214, and Nup358, were observed to be phosphorylated throughout the cell cycle and hyperphosphorylated at mitosis, whereas a fourth nucleoporin, p62, was not phosphorylated at all [28]. These studies suggest that certain nucleoporins undergo differential phosphorylation during the cell cycle, but a temporal correlation of the phosphorylation status of these proteins and their association with the nuclear envelope during mitosis has not been firmly established.

In the present work, we have examined the mitotic distribution of a nuclear-pore-associated protein that is phosphorylated during mitosis. We have earlier described a monoclonal antibody, mAb E2, that specifically inhibited the signal-mediated import of an exogenous protein in nuclear transport assays performed with digitonin-permeabilized F-111 rat fibroblast cells and recognized proteins putatively localized in nuclear pores by biochemical fractionation studies [29]. In this study we show that mAb E2 recognizes a 58-kDa protein in F-111 rat fibroblast cells which is partially associated with NPC proteins recognized by mAb 414 by confocal microscopy. Biochemical studies indicate that this 58-kDa protein does not belong to the major class of nucleoporins that are modified by *N*-acetylglucosamine residues. This nuclear-pore-associated protein, termed NPA58, is specifically phosphorylated during mitosis. There is complete dephosphorylation of NPA58 upon release from metaphase arrest. Studies with mitotic cells indicate that NPA58 is dispersed in the cytoplasm during the early stages of mitosis when it is phosphorylated. The relocalization of NPA58 in the reassembled nuclear envelope in telophase cells temporally correlates with its dephosphorylation upon release from metaphase arrest. These results firmly support the role of phosphorylation and dephosphorylation in the dissociation and reassociation of components of the NPC during mitosis.

MATERIALS AND METHODS

Cell culture and labeling. F-111 rat lung fibroblast cells were routinely maintained in Dulbecco's minimum essential medium (DMEM) supplemented with 10% fetal calf serum (FCS). To obtain cells arrested in mitosis, cells were grown to 70% confluency and treated with 0.01% nocodazole (Sigma Chemical Co., St. Louis, MO) in the culture medium for 12–14 h. The metaphase-arrested cells were collected as the nonadherent population, washed in DMEM, reseeded in fresh DMEM supplemented with 10% FCS at 37°C, and harvested or fixed at appropriate times. For radiolabeling cells in culture, a subconfluent population of F-111 cells was starved for 2–3 h in phosphate-free or methionine-free DMEM. Cells were labeled for 12–14 h in the presence of 10% FCS with 100 μCi/ml [^{35}S]methionine (1000 Ci/mmol, New England Nuclear, Boston, MA) or 400 μCi/ml [^{32}P]orthophosphoric acid (6000 Ci/mmol, Board of Radiation and Isotope Technology, Mumbai, India). To obtain labeled metaphases, cells were labeled in the presence of 0.01% nocodazole and the mitotic population was collected as described above.

Antibodies. Mouse mAb E2 has been described previously [29]. The hybridoma supernatants were used directly in immunoblot analysis or concentrated 10- or 2-fold for immunofluorescence and immunoprecipitation assays respectively. LB-P, a rabbit polyclonal antibody to recombinant rat lamin B1, has been described earlier [30]. A rabbit polyclonal antibody to U5-116 kDa [31] was a gift from Dr. R. Lührmann (University of Marburg, Germany). MAb 414, a mouse monoclonal antibody which recognizes a class of NPC proteins [32], was obtained from Berkeley Antibody Co. (Richmond, CA). All antibodies were used at the recommended dilutions for immunofluorescence assays and immunoblot analysis. MAb 414 was biotinylated by coupling with excess *N*-hydroxysuccinimidobiotin (Sigma Chemical Co.) in 0.1 M sodium borate buffer, pH 8.8, using standard procedures.

Immunofluorescence microscopy. F-111 cells were grown on coverslips to about 70% confluency prior to fixing, or nocodazole-arrested metaphase cells were collected and seeded on coverslips as described above and fixed at appropriate times. The cells were fixed with 3.7% formaldehyde for 10 min and permeabilized with 0.5% Triton X-100 for 5 min at room temperature for immunolabeling with mAb E2 and mAb 414. Alternatively cells were also fixed with methanol:acetone (2:1, v/v) at 4°C for 15 min for immunolabeling with LB-P. Further processing was carried out at room temperature. Cells were blocked with 3% BSA for 1–2 h, incubated with the primary antibody for 1–2 h, and then secondary antibody conjugated to FITC or Alexa 488 for 1 h. For double labeling studies with mAb E2 and mAb 414, cells were fixed, blocked, and incubated serially with mAb E2, followed by Alexa 488-conjugated anti-mouse antibody, and then with biotinylated mAb 414 followed by avidin–Cy3. In a control experiment, when fixed F-111 cells were incubated with biotinylated mAb 414 followed by Alexa 488-conjugated anti-mouse antibody no signal was obtained, indicating that the biotinylated antibody was unable to bind to the anti-mouse antibody and excluding the possibility that free antigen-binding sites in the anti-mouse antibody could bind to biotinylated mAb 414 to give false colocalization. Secondary antibody conjugates were from Molecular Probes (Eugene, OR), Jackson Immunoresearch Laboratories (West Grove, PA), and Vector Laboratories (Burlingame, CA) and used at the recommended dilutions. Coverslips were mounted in Vectashield (Vector Laboratories) containing 1 μg/ml 4,6-diamidino-2-phenylindole (DAPI). All samples were routinely viewed under phase contrast also. Confocal laser-scanning immunofluorescence microscopy (CLSM) was carried out on a Meridian Ultima scan head attached to an Olympus IMT-2 inverted microscope fitted with a 60×, 1.4 NA objective lens, with

excitation at 515, 488, and 351–364 nm (argon–ion laser). The 351–364 nm laser was used for excitation of DAPI, with a 485/40 bandpass filter for detection. The 488-nm laser was used for excitation of dye conjugates, with a 560-nm shortpass dichroic, a 530/30 bandpass filter for detection of FITC and Alexa 488, and a 580/30 bandpass filter for the detection of Cy3. In double labeling experiments, the percentage crossover for each dye was calculated automatically after scanning singly labeled specimens under identical settings using Ultima master program V 4.15 and corrected for during image analysis. Images were analyzed using DASY master program V4.19 (Meridian Instruments Inc., Okemos, MI) and assembled using Adobe Photoshop 5.0.

Cell fractionation and immunoblot analysis. Cell fractionation was carried out as described previously [33]. Briefly, 70–80% confluent F-111 cells grown in 10-cm petri dishes were rinsed twice in phosphate-buffered saline containing 2 mM $MgCl_2$ and once with MOPS buffer (50 mM Mops–NaOH, pH 7.0, 1 mM EGTA, 5 mM $MgCl_2$, and 1 mM PMSF in ethanol) at room temperature. Subsequent steps were performed at 4°C using ice-cold solutions. Cells were extracted *in situ*, first with 2 ml Mops buffer containing 0.2% Triton X-100 for 5 min, briefly washed with 2 ml Mops buffer, and then extracted for 5 min in 2 ml Mops containing 500 mM NaCl, again followed by a brief washing with Mops buffer. The residual cellular proteins that remained in the petri dishes were immediately scraped off in 0.5 ml of Laemmli buffer and boiled. Soluble proteins recovered after each fractionation and washing were combined, cleared by centrifugation at 13,000*g* at 4°C for 10 min, and precipitated from the supernatant with 4 vol of ice-cold methanol overnight at −20°C. Unfractionated F-111 cells were harvested and lysed directly in Laemmli buffer ($4–5 \times 10^6$ cells/ml) or cell extracts were immunoprecipitated as described in the next section. Equivalent amounts of cell fractions, total cell lysates, or immunoprecipitates were separated by SDS–PAGE and electroblotted onto PVDF membranes (Millipore, Bedford, MA). Immunodetection was carried out using standard protocols [29] with antibodies diluted appropriately. Color reaction was developed using nitroblue tetrazolium and 5-bromo-4-chloro-indolyl phosphate as substrate for alkaline phosphatase-conjugated secondary antibodies or chemiluminescence was detected using an ECL detection kit (Amersham Inc., UK) for HRP-conjugated secondary antibodies as per the manufacturer's instructions. For wheat germ agglutinin (WGA)-binding studies, WGA was coupled to CNBr-activated Sepharose 6B as per the manufacturer's instructions (Pharmacia Fine Chemicals, Uppsala, Sweden). F-111 cells were lysed in binding buffer (20 mM Hepes, pH 7.3, 200 mM KCl, 2 mM $MgCl_2$, 2 mM DTT, 1% Triton X-100, 0.1 mM sodium orthovanadate, 1 μg/ml each of aprotinin, pepstatin, and leupeptin) for 30 min at 4°C ($4–5 \times 10^6$ cells/ml) as described [34]. The lysate was centrifuged and the supernatant was incubated with WGA–Sepharose for 2–3 h at 4°C. A control binding experiment was carried out with WGA–Sepharose in the presence of 0.4 M *N*-acetylglucosamine. After incubation, the WGA–Sepharose samples were washed extensively with binding buffer, boiled in Laemmli buffer, separated by SDS–PAGE, and electroblotted onto PVDF membranes for immunoblot analysis.

Immunopreciptation assays. F-111 cells (about 5×10^6 cells/ml) were lysed in RIPA buffer (50 mM Tris–HCl, pH 7.4; 0.5% Triton X-100; 0.1% SDS; 0.5% Na–deoxycholate; 150 mM NaCl; 1mM DTT; 1 mM PMSF; 1 μg/ml each of aprotinin, leupeptin, and pepstatin; 5 mM EDTA; 50 mM NaF; 1 mM Na–orthovanadate) on ice for 10 min. Lysates were passed 8–10 times through a 1-ml syringe fitted with a 22-gauge needle to shear DNA, centrifuged at 10,000*g* for 15 min at 4°C to remove cellular debris, and precleared with 10 μl of protein G–Sepharose per milliliter of lysate for 1 h at 4°C. Precleared lysates were immunoprecipitated with protein G–Sepharose beads (20–30 μl beads/ml lysate), which were preincubated with appropriate antibodies at 4°C for 2 h. Control immunoprecipitation reactions were carried out with protein G–Sepharose preincubated with buffer alone (for mAb 414) or with hybridoma medium containing 10% FCS but without mAb (for mAb E2). The immunoprecipitates were washed 4–6 times with 1 ml RIPA buffer, boiled in Laemmli buffer, and analyzed by SDS–PAGE and immunoblotting. Radiolabeled samples were analyzed by autoradiography. For alkaline phosphatase treatment of samples, immunoprecipitates were washed thrice in reaction buffer (20 mM Tris–HCl, pH 7.4, 5 mM $MgCl_2$, and protease inhibitors) followed by treatment with 10 U of calf intestinal alkaline phosphatase (New England Biolabs) in 100 μl reaction buffer at 37°C for 30 min. A control reaction was carried out in the presence of 5 mM Na–orthovanadate as an inhibitor of phosphatase. The reaction was stopped by adding Laemmli buffer and analyzed by SDS–PAGE and immunoblotting. For alkali treatment of immunoblotted samples, the PVDF membrane was treated with 1 M NaOH for 1 h at 55°C. The blot was rinsed several times in 10 mM tetrasodium pyrophosphate and autoradiographed.

RESULTS

Biochemical Characterization of NPA58

Our earlier data from fractionation of rat liver nuclear envelopes suggested that the antigens recognized by mAb E2 were associated with the nuclear pore complexes, and we had observed that mAb E2 could specifically inhibit the import of nuclear substrates in semi-intact F-111 rat lung fibroblast cells [29]. In order to characterize the mAb E2-reactive protein in F-111 cells with respect to other known nuclear pore complex proteins, whole cell lysates of F-111 cells were analyzed by immunoblotting as described under Materials and Methods. MAb E2 recognized a single protein of 58 kDa in F-111 cell lysates, as shown in Fig. 1A. The lysates were also analyzed with mAb 414, a monoclonal antibody which is known to recognize a family of related nucleoporins of sizes 62, 153, 214, and 358 kDa [28, 32]. It was evident that NPA58 migrated as a species distinct from those recognized by mAb 414. In order to confirm the specificity of mAb E2, immunoprecipitation assays were carried out with [^{35}S]methionine-labeled F-111 cell extracts and mAb E2. As illustrated in Fig. 1B, only a single species of 58 kDa was detected by autoradiography and the identity of the immunoprecipitate was confirmed by immunoblotting the same sample with mAb E2. The experiment also confirmed that there were no detectable levels of coprecipitating antigens observed under the conditions described. We also carried out two-dimensional IEF–SDS–PAGE and ascertained that the immunoprecipitated sample contained a single species migrating at p*I* 5.8–5.9 and M_r 58 kDa (data not shown). Cultured F-111 cells were subjected to biochemical fractionation *in situ* followed by immunoblot analysis of the fractions with mAb E2 and mAb 414 to determine the cellular localization of the antigens. NPA58 was predominantly retained in the detergent- and salt-insoluble pellet, though a significant amount was solubilized with Triton X-100 or 0.5 M NaCl (see Fig. 1C). Of the mAb 414-reactive proteins, p62 and Nup214 exhibited a similar profile to that of NPA58 whereas Nup153 was resistant to detergent extraction

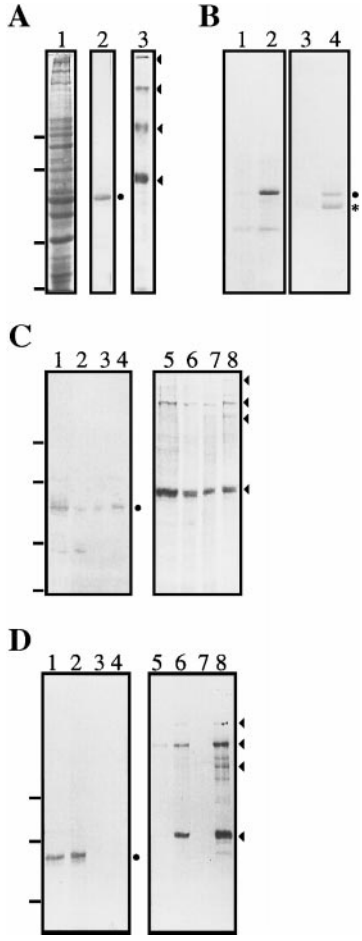

FIG. 1. Biochemical characterization of NPA58. (A) F-111 cell extracts ($2–3 \times 10^5$ cells) were separated by SDS–PAGE and stained with Coomassie blue (lane 1) or immunoblotted with mAb E2 (lane 2) or mAb 414 (lane 3). (B) Extracts from F-111 cells labeled with [^{35}S]methionine were immunoprecipitated with hybridoma medium as control and with mAb E2 and analyzed by autoradiography (lanes 1 and 2) or by immunoblotting with mAb E2 (lanes 3 and 4). (C) F-111 cells were fractionated as described and the same percentage of proteins from each fraction was analyzed by immunoblotting with mAb E2 (lanes 1–4) or mAb 414 (lanes 5–8): unfractionated cell lysate (lanes 1 and 5); 0.2% Triton X-100 supernatant (lanes 2 and 6); 500 mM NaCl supernatant (lanes 3 and 7); and residual cellular proteins (lanes 4 and 8). (D) F-111 cell lysates were incubated with WGA–Sepharose and equivalent aliquots were analyzed by immunoblotting with mAb E2 (lanes 1–4) or mAb 414 (lanes 5–8): unbound fraction (lanes 1 and 5); total lysate (lanes 2 and 6); bound fraction (lanes 4 and 8); and fraction bound in the presence of 0.4 M *N*-acetylglucosamine (lanes 3 and 7). The molecular mass markers are indicated by dashes to the left of the panels and from top to bottom represent phosphorylase B (94 kDa), albumin (67 kDa), ovalbumin (43 kDa), and carbonic anhydrase (30 kDa). The dots indicate the positions of NPA58, arrowheads indicate the mAb 414-reactive antigens and asterisks denote the mouse IgG bands.

and Nup358 appeared resistant to both detergent and salt extraction.

Several nucleoporins including the mAb 414-reactive proteins and the p62 complex are modified by O-linked *N*-acetylglucosamine residues and hence bind to the lectin WGA [35, 36]. In order to determine whether NPA58 could bind to WGA, F-111 cell lysate was incubated with WGA–Sepharose and the bound and unbound fractions were analyzed by SDS–PAGE followed by immunoblotting with mAb E2 or mAb 414. As shown in Fig. 1D, NPA58 was retained in the unbound fraction and did not bind at all to WGA–Sepharose (lanes 1–4). On the other hand, the mAb 414-reactive proteins bound efficiently to WGA–Sepharose (lanes 5–8). This binding was specific as it did not occur in the presence of 0.4 M *N*-acetylglucosamine. Thus NPA58 is unable to bind WGA and is therefore distinct from the nucleoporins that are modified by O-linked *N*-acetylglucosamine residues.

Intracellular Localization of NPA58

In order to determine the intracellular distribution of NPA58 in normal and mitotic cells, F-111 cells were immunolabeled with mAb E2 and mAb 414 and stained for DNA with DAPI. In interphase cells, both mAb E2 and mAb 414 stained the nuclear rim in a punctate pattern, with a high degree of coincident immunofluorescence as seen in the merged panel (Figs. 2A–2C). By prometaphase both NPA58 and the mAb 414-reactive NPC proteins were completely dissociated from the nuclear envelope and localized largely in the cytoplasm. In metaphase cells the distribution of NPA58 was entirely cytoplasmic and completely excluded from the mitotic apparatus unlike the localization of PBC68, a nuclear pore protein which associates reversibly with the mitotic spindle [37]. The cytoplasmic staining was observed in all the early stages of mitosis until anaphase, and there was no appearance of either protein in association with the chromosomes until this stage. By late anaphase or early telophase, NPA58 had begun localizing around the chromatin producing a marked rim-like appearance. A corresponding clustering of NPC proteins around the chromatin was observed in the same cell. The merged image showed that both NPA58 and the mAb 414-reactive proteins were localized within the same region at this early stage of nuclear envelope formation (Fig. 2S). By late telophase the NPC proteins as well as NPA58 were completely incorporated within the nuclear envelope as seen in Figs. 2U–2W. The topology of the nascent nuclear envelope was generally uneven and the nuclei appeared more rounded only by cytokinesis when envelope formation was complete.

Phosphorylation of NPA58 during Mitosis

In initial experiments designed to explore the possibility that NPA58 might be phosphorylated, F-111 cells were labeled with [^{32}P]orthophosphoric acid and cell lysates were immunoprecipitated with mAb E2. As

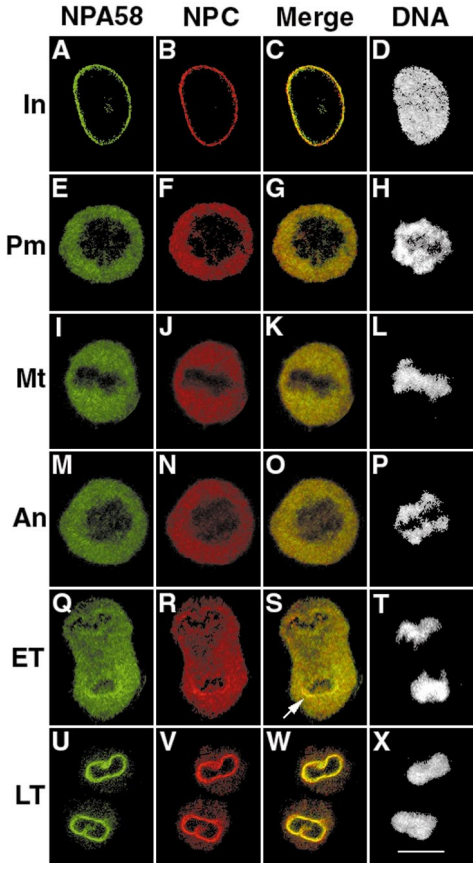

FIG. 2. Distribution of NPA58 and NPC proteins during mitosis. Formaldehyde-fixed F-111 cells were stained with mAb E2 (NPA58) and mAb 414 (NPC) and counterstained for DNA, and cells in various stages of mitosis were examined. (A–D) Interphase, In; (E–H) prometaphase, Pm; (I–L) metaphase, Mt; (M–P) anaphase, An; (Q–T) early telophase, ET; (U–X) late telophase, LT. Arrow in S indicates the coincident immunofluorescence of NPA58 and mAb 414-reactive NPC proteins in the reforming nuclear envelope in early telophase. Bar, 10 μM.

shown in Fig. 3A, two closely spaced phosphorylated forms of NPA58 were observed (lane 1). Comparison of the intensity of the phosphorylation signal with the amount of protein immunoprecipitated (lanes 1 and 3) indicated that the phosphorylation of the slower migrating form was six- to sevenfold higher than that of the faster migrating form. The amount of the slower migrating form in the immunoblot was much lower (five- to sixfold) than the faster migrating form and was detectable only on overloading of the extract from exponentially growing cells, as in this experiment. Treatment of the samples with alkaline phosphatase removed almost all the radioactive signal and resulted in disappearance of the slower migrating form (lanes 2 and 4). This suggested that phosphorylation of NPA58 retarded its electrophoretic mobility, and this was confirmed in the following set of experiments.

As the phosphorylation of various nuclear envelope proteins during mitosis is well documented [38], we checked whether NPA58 was phosphorylated in mitotic cells by comparing immunoblots of mitotic cells isolated by shake-off from F-111 subconfluent cultures and the residual adherent interphase cells. The mitotic population consisted of ~60% metaphase cells and the remaining cells were found to be in other mitotic stages when viewed under a bright-field microscope. As seen from Fig. 3B, NPA58 showed both a slower and a faster migrating form in mitotic cell extracts (lane 2) and only the faster migrating form in interphase cells (lane 1). In order to obtain a higher percentage of cells in metaphase, F-111 cells were treated with the drug nocodazole, which is known to inhibit spindle assembly, is nontoxic at low concentrations, and causes reversible metaphase arrest of cells [39, 40]. This treatment yielded >80% of mitotic cells arrested in metaphase in the nonadherent population. Immunoblot analysis of nocodazole-treated cells indicated that the mobility of NPA58 from the metaphase-arrested cells was com-

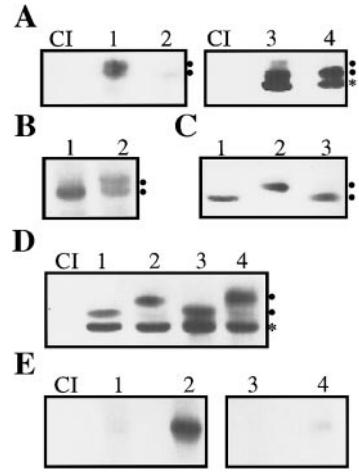

FIG. 3. Phosphorylation of NPA58 in F-111 cell extracts. (A) NPA58 was immunoprecipitated from ^{32}P-labeled F-111 cell extracts ($4–5 \times 10^6$ cells) and analyzed by autoradiography before and after treatment with alkaline phosphatase (lanes 1 and 2). Lanes 3 and 4, the immunoblot analysis of the same samples with mAb E2. (B) Immunodetection of NPA58 in whole cell extracts ($2–3 \times 10^5$ cells) made from interphase (lane 1) and mitotic cells (lane 2). (C) Immunoblot analysis of NPA58 in whole cell extract ($2–3 \times 10^5$ cells) made from interphase (lane 1), nocodazole-arrested (lane 2), and adherent (lane 3) F-111 cells. (D) Immunoprecipitates of NPA58 from F-111 cells ($1.5–2.0 \times 10^6$ cells) in interphase (lane 1), cells arrested with nocodazole (lane 2), immunoprecipitates of nocodazole-arrested cells treated with alkaline phosphatase in the absence or presence of vanadate (lanes 3 and 4) were immunoblotted with mAb E2. (E) Autoradiograms of ^{32}P-labeled immunoprecipitates of NPA58 from interphase and nocodazole-arrested F-111 cells before (lanes 1and 2) and after (lanes 3 and 4) treatment with alkali. The dots on the right side of the panels indicate the two differentially phosphorylated forms of NPA58, the mouse IgG band is indicated by an asterisk, and lanes marked CI correspond to negative control immunoprecipitations carried out with cell extract and hybridoma medium without the primary mouse mAb.

pletely retarded compared to the adherent interphase cells or untreated exponentially growing cells (Fig. 3C, lanes 1–3). Treatment of the immunoprecipitate from metaphase-arrested cells with alkaline phosphatase reversed the mobility shift (Fig. 3D, lanes 1–3) which was inhibited in the presence of the phosphatase inhibitor, Na–orthovanadate (lane 4). This confirmed that the retarded mobility of NPA58 in mitotic cells was due to phosphorylation. In order to check whether the phosphorylation of NPA58 was at Ser/Thr residues (alkali-labile modification), an immunoblot of NPA58 immunoprecipitated from labeled metaphase-arrested cells was treated with alkali as described. Most of the signal in the mitotic immunoprecipitate was observed to be labile to alkali treatment (Fig. 3E), suggesting that NPA58 is a substrate for a mitotic Ser/Thr kinase.

Stability of Mitotic Phosphorylation of NPA58

The phosphorylation of NPA58 was further analyzed to determine its stability during the early and later stages of mitosis. To examine the steady-state phosphorylation of NPA58 in mitotic cells, metaphase-arrested cells labeled with [^{32}P]orthophosphoric acid were chased in unlabeled medium for 2 h in the presence of nocodazole. Analysis of the immunoprecipitates showed that although there was considerable turnover of phosphate in the mitotic cytosol (Fig. 4A, lanes 2 and 3), NPA58 displayed retarded electrophoretic mobility through the chase period (Fig. 4A, lanes 5 and 6), indicating that there was no change in the overall phosphorylation state of the protein during metaphase. We then examined the phosphorylation of NPA58 in cells released from metaphase arrest by immunoprecipitating extracts made from ^{32}P-labeled metaphase cells that were reseeded in unlabeled medium in the absence of nocodazole and harvested over a period of 2 h. As shown in Fig. 4B, the mitotic immunoprecipitate was highly phosphorylated, but within 1 h of release from metaphase arrest, NPA58 was completely dephosphorylated. This was accompanied by a corresponding change in its electrophoretic mobility as seen in the immunoblot analysis of the same samples. Since the immunoreactivity of NPA58 was maintained in both the above experiments, this confirmed that the dephosphorylation of NPA58 was not accompanied by its degradation. In order to study the time course of dephosphorylation of NPA58 for a longer period, whole cell lysates of cells released from metaphase arrest were analyzed by immunoblotting. As seen in Fig. 4C, NPA58 was detected as the slow-migrating, phosphorylated form during the early stages of release. At 30 min, there was a partial conversion to the faster migrating form. By 1 h of release from the arrest, NPA58 was quantitatively shifted to the faster migrating form representing the dephosphorylated state of the protein.

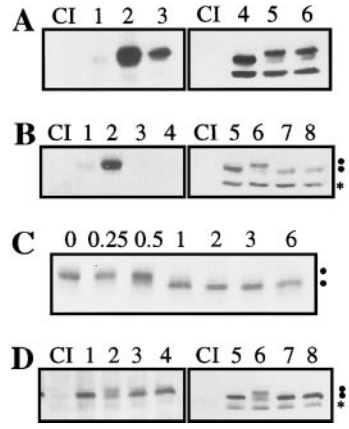

FIG. 4. Dephosphorylation of NPA58 in cells released from metaphase arrest. (A) Immunoprecipitates of NPA58 from ^{32}P-labeled adherent F-111 cells (lane 1) and metaphase-arrested cells before and after chase in unlabeled medium for 2 h (lanes 2 and 3) were analyzed by autoradiography, followed by immunoblotting with mAb E2 (lanes 4–6). (B) Immunoprecipitates of NPA58 from [^{32}P]-labeled adherent F-111 cells (lane 1) or cells that were released from metaphase-arrest for 0 h (lane 2), 1 h (lane 3) and 2 h (lane 4) were analyzed by autoradiography followed by immunoblotting with mAb E2 (lanes 5–8). (C) Immunoblot analysis of F-111 cells released from metaphase arrest over a period of 0–6 h. (D) Immunoprecipitates of NPA58 from [^{35}S]methionine-labeled adherent F-111 cells or metaphase-arrested cells and cells that were allowed to exit from the arrest for 1 and 2 h were autoradiographed (lanes 1–4) and also immunoblotted with mAb E2 (lanes 5–8). The dots to the side of the panels indicate the two phosphorylated forms of NPA58, the asterisk denotes the mouse IgG band, and the lanes marked CI correspond to negative control immunoprecipitation reactions carried out with cell extract and hybridoma medium without the primary mouse mAb.

Earlier studies have established that NPC assembly does not require new protein synthesis [41], indicating that NPC components are stably present in the mitotic cytoplasm and recycled after mitosis. We examined the stability of NPA58 protein in the mitotic precursor pool by analyzing immunoprecipitates of cells that were labeled with [^{35}S]methionine overnight in the presence of nocodazole followed by a chase in unlabeled medium in the absence of nocodazole to allow exit from metaphase. As shown in Fig. 4D, ^{35}S-labeled NPA58 was not degraded during the chase period. The slow-migrating form of the labeled protein in metaphase extracts reverted completely to the form having faster electrophoretic mobility upon dephosphorylation as expected. From the above experiments it can be concluded that NPA58 is phosphorylated in metaphase-arrested cells but is dephosphorylated upon exit from metaphase arrest, and the protein remains a stable component of the mitotic precursor pool.

Localization of NPA58 during Nuclear Reassembly

In order to examine the distribution of NPA58 during nuclear reassembly, immunolocalization studies

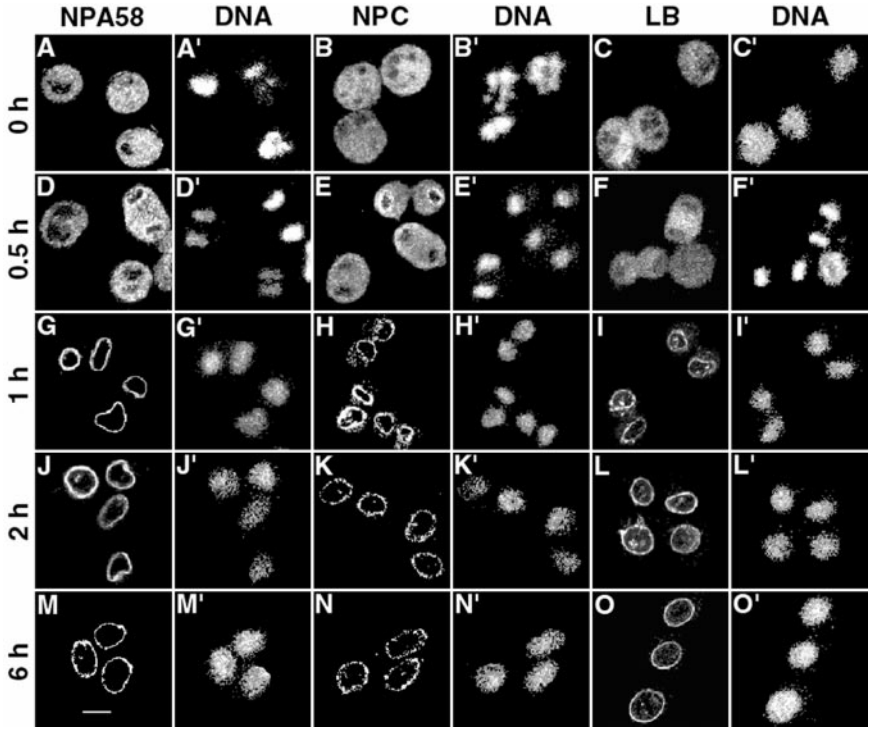

FIG. 5. Localization of NPA58 and nuclear antigens in cells released from metaphase arrest. (A–O) Metaphase-arrested F-111 cells were released over a period of 0–6 h, fixed, and immunostained with appropriate antibodies to visualize NPA58, mAb 414-reactive NPC proteins (NPC), and lamin B1 (LB) at the indicated times. The DNA profile of the cells is represented in the adjacent columns (A′–O′). Bar, 10 μm.

were performed with cells arrested and released from metaphase, using mAb 414 as a marker for pore assembly and an antibody to lamin B1 to follow envelope reformation. We observed that NPA58 was entirely cytoplasmic in nocodazole-arrested cells (Fig. 5A). The cytoplasmic localization correlated well with the phosphorylation of NPA58 in these cells. The mAb 414-reactive NPC proteins (Fig. 5B) as well as lamin B1 (Fig. 5C) were similarly observed to be cytoplasmic. At 30 min of release from the arrest (Figs. 5D–5F), NPA58 had begun to associate with the reforming nuclear envelope in cells that had progressed till early telophase (~30% of the population), while the remaining cells showed only cytoplasmic staining of NPA58. Similar observations were recorded with mAb 414 at this time point. Lamin B1 continued to be cytoplasmic in its distribution even at 30 min of release from nocodazole arrest. At 1 h of release from the arrest (Figs. 5G–5I), more than 75% of the cells were in telophase and NPA58 was entirely associated with the nuclear envelope. This observation was highly significant in correlating the phosphorylation status of NPA58 with its association with the nuclear envelope since in the previous section we had demonstrated that NPA58 was dephosphorylated by 1 h of release of cells from metaphase arrest. The NPC proteins recognized by mAb 414 were also localized in the nuclear envelope in telophase cells at 1 h of release. At this time the nuclear lamin B1 appeared as a rim at the periphery of the nucleus. By 2 h of release from metaphase arrest, the cells had completed cytokinesis and by 6 h the cells had attained normal fibroblast-like morphology and NPA58, the mAb 414-reactive NPC proteins as well as lamin B1 were completely incorporated in the nuclear envelope (Figs. 5J–5O).

Although the nocodazole-treated cells took considerably longer than normal cells to traverse the different stages of mitosis after release from metaphase arrest, the majority of the cells crossed mitosis normally. We observed that U5-116 kDa, a nucleoplasmic protein, which remained cytoplasmic in the early stages of release from metaphase arrest, started accumulating inside the nucleus at 1 h of release in $>$ 90% of cells when both NPA58 and mAb 414-reactive NPC proteins were associated with the nuclear region and lamin B1 was also targeted to the nucleus.

DISCUSSION

In this study we have conducted a detailed investigation of the phosphorylation/dephosphorylation of NPA58 during the cell cycle and correlated this to its intracellular distribution. NPA58 undergoes mitosis-specific phosphorylation in the early stages of mitosis

when it is dispersed in the cytoplasm of the cell. Dephosphorylation of NPA58 occurs *in vivo* upon exit from metaphase arrest and temporally correlates with the localization of the protein to the reforming nuclear envelope. The protein remains a stable component of the mitotic precursor pool during its phosphorylation and dephosphorylation. Moreover, the distribution of NPA58 during the various stages of mitosis as well as during the assembly of the nuclear envelope closely correlates with that of NPC proteins recognized by mAb 414.

NPA58 Is Associated with the Nuclear Pore Complex

The association of NPA58 with the NPC is supported by the following lines of evidence. First, the immunolocalization of this protein in F-111 cells by confocal microscopy showed a characteristic punctate staining at the nuclear periphery in interphase cells, which was highly coincident with that displayed by mAb 414, a monoclonal antibody to a well-characterized class of nucleoporins [32]. Second, further evidence for the association of NPA58 with the NPC was obtained from studying its distribution in mitotic cells. The protein was dispersed in the cytoplasm until anaphase and did not show any significant association with chromatin until this stage. By early telophase, NPA58 started to localize around the condensed chromatin. At this stage both the mAb 414-reactive NPC proteins and NPA58 appeared concentrated around the chromatin region in the reforming nuclear envelope. The localization of NPA58 in association with the pores is consistent with our earlier evidence on the specific inhibition of signal-mediated import of proteins in semi-intact F-111 cells by mAb E2 [29].

Phosphorylation of NPA58 Correlates with Its Mitotic Distribution

The disassembly of the nuclear envelope is initiated at late prophase or early prometaphase following the phosphorylation of the nuclear lamins by $p34^{cdc2}$ kinase [21, 22]. The integral membrane proteins are also reversibly phosphorylated during mitosis and this regulates their association with lamin proteins and chromosomes [23, 24, 42, 43]. The mitosis-specific phosphorylation of certain NPC proteins such as *Xenopus* p97 and p200, and mammalian gp210, and the mitotic hyperphosphorylation of Nup153, Nup214, and Nup358 have been reported, though p62 is not phosphorylated at all [27, 28]. In this study we have demonstrated that NPA58, a pore-associated protein, is phosphorylated in metaphase cells when it is dispersed in the cytoplasm of the cell subsequent to nuclear envelope breakdown. When metaphase-arrested cells were allowed to complete mitosis, NPA58 was observed to be completely dephosphorylated within 1 h. We observed NPA58 to relocalize to the nuclear region in cells released from metaphase arrest for the same period and this provides evidence that the dephosphorylation of NPA58 temporally correlates with its association with the reforming nuclear envelope. This is a significant finding because protein dephosphorylation preceding or concomitant with recruitment to the chromatin region has not been documented so far for any of the known NPC proteins. Phosphorylation–dephosphorylation events are likely to regulate higher order interactions among the NPC components and might also be significant in regulating their association with chromatin or nuclear membranes and in defining the order of their recruitment in the NPC at the close of mitosis.

Localization of NPA58 during Nuclear Envelope Assembly

The three major events that are required for the assembly of a functional nucleus include attachment and fusion of nuclear vesicles and cisternae, assembly of NPCs on fused membranes, and repolymerization of the nuclear lamina [20, 43]. The association of nuclear membranes with the chromosome surface and incorporation of inner membrane proteins such as LAP2 and LBR precedes NPC assembly [25, 26, 42, 44, 45]. The assembly of the pore complex can be distinguished into biochemically distinct steps [46] and proceeds through a series of intermediate structures that have been visualized in ultrastructural studies on nuclear envelope assembly [47] suggesting a requirement for sequential and ordered reassembly of the various NPC components. More recently, it has been observed that NPC reassembly begins in a stepwise manner in late anaphase or early telophase with recruitment of Nup153, POM121, p62, and Nup214 followed finally by gp210 and Tpr 270 in late telophase [48]. In this study we have observed that NPA58 associates with the nuclear region during early telophase, overlapping with the relocalization of mAb 414-reactive NPC proteins.

At present the primary structure of NPA58 and its sequence relationships with known nucleoporins are not clear. However, from its molecular mass and inability to bind to WGA, NPA58 appears to be a novel protein that is partially associated with the NPCs. It is interesting to note that during mitosis, NPA58 is incorporated into the reforming nuclear envelope at an early stage when the mAb 414-reactive proteins are reassembled. Most importantly, the dissociation and reassociation of NPA58 with the nuclear envelope closely follows its phosphorylation and dephosphorylation during mitosis, suggesting that these modifications are essential for its mitotic localization.

We thank Dr. R. Lührmann for gift of the antibody to U5-116 kDa, and Dr. M. R. S. Rao for helpful discussions. We are grateful to

Nandini Rangaraj for expert assistance with confocal microscopy and V. K. Sharma and N. R. Chakrabarthi for upkeep of the confocal microscope.

REFERENCES

1. Gerace, L., and Burke, B. (1988). Functional organization of the nuclear envelope. *Annu. Rev. Cell Biol.* **4,** 335–374.
2. Forbes, D. J. (1992). Structure and function of the nuclear pore complex. *Annu. Rev. Cell Biol.* **8,** 495–527.
3. Feldherr, C. M., and Akin, D. (1994). Role of nuclear trafficking in regulating cellular activity. *Int. Rev. Cytol.* **151,** 183–228.
4. Fabre, E., and Hurt, E. C. (1994). Nuclear transport. *Curr. Opin. Cell Biol.* **6,** 335–342.
5. Görlich, D., and Mattaj, I. W. (1996). Nucleocytoplasmic transport. *Science* **271,** 1513–1518.
6. Nigg, E. A. (1997). Nucleocytoplasmic transport: Signals, mechanisms and regulation. *Nature* **386,** 779–787.
7. Nakielny, S., and Dreyfuss, G. (1999). Transport of proteins and RNAs in and out of the nucleus. *Cell* **99,** 677–690.
8. Görlich, D., and Kutay, U. (1999). Transport between the cell nucleus and the cytoplasm. *Annu. Rev. Cell Dev. Biol.* **15,** 607–660.
9. Akey, C. W., and Radermacher, M. (1993). Architecture of the *Xenopus* nuclear pore complex revealed by three dimensional cryo-electron microscopy. *J. Cell Biol.* **122,** 1–20.
10. Panté, N., and Aebi, U. (1995). Toward a molecular understanding of the structure and function of the nuclear pore complex. *Int. Rev. Cytol.* **162,** 225–255.
11. Yang, Q., Rout, M. P., and Akey, C. W. (1998). Three-dimensional architecture of the isolated yeast nuclear pore complex: Functional and evolutionary implications. *Mol. Cell* **1,** 223–234.
12. Reichelt, R., Holzenburg, A., Buhle, E. L., Jarnik, M., Engel, A., and Aebi, U. (1990). Correlation between structure and mass distribution of the nuclear pore complex and of distinct pore components. *J. Cell Biol.* **110,** 883–894.
13. Jarnik, M., and Aebi, U. (1991). Toward a more complete 3-D structure of the nuclear pore complex. *J. Struct. Biol.* **107,** 291–308.
14. Goldberg, M. W., and Allen, T. D. (1992). High resolution scanning electron microscopy of the nuclear envelope: Demonstration of a new regular fibrous lattice attached to the baskets of the nucleoplasmic face of the nuclear pores. *J. Cell Biol.* **119,** 1429–1440.
15. Panté, N., and Aebi, U. (1996). Sequential binding of import ligands to distinct nucleopore regions during their nuclear import. *Science* **273,** 1729–1732.
16. Ris, H. (1991). The 3-D structure of the nuclear pore complex as seen by high-voltage electron microscopy and high resolution low voltage scanning electron microscopy. *EMSA Bull.* **21,** 54–56.
17. Rout, M. P., Aitchison, J. D., Suprapto A., Hjertaas, K., Zhao Y., and Chait, B. T. (2000). The yeast nuclear pore complex: Composition, architecture, and transport mechanism. *J. Cell Biol.* **148,** 635–652.
18. Doyé, V., and Hurt, E. (1997). From nucleoporins to nuclear pore complexes. *Curr. Opin. Cell Biol.* **9,** 401–411.
19. Stoffler, D., Fahrenkrog, B., and Aebi, U. (1999). The nuclear pore complex: From molecular architecture to functional dynamics. *Curr. Opin. Cell Biol.* **11,** 391–401.
20. Gant, T. M., and Wilson, K. L. (1997). Nuclear assembly. *Annu. Rev. Cell Dev. Biol.* **13,** 669–695.
21. Peter, M., Nakagawa, J., Doree, M., Labbe, J. C., and Nigg, E. A. (1990). In vitro disassembly of the nuclear lamina and M phase-specific phosphorylation of lamins by cdc2 kinase. *Cell* **61,** 591–602.
22. Heald, R., and McKeon, F. (1990). Mutations of phosphorylation sites in lamin A that prevent nuclear lamina disassembly in mitosis. *Cell* **61,** 579–589.
23. Appelbaum, J., Blobel, G., and Georgatos, S. D. (1990). In vivo phosphorylation of the lamin B receptor. Binding of lamin B to its nuclear membrane receptor is affected by phosphorylation. *J. Biol. Chem.* **265,** 4181–4184.
24. Foisner, R., and Gerace, L. (1993). Integral membrane proteins of the nuclear envelope interact with lamins and chromosomes, and binding is modulated by mitotic phosphorylation. *Cell* **73,** 1267–1279.
25. Yang, L., Guan, T., and Gerace, L. (1997). Integral membrane proteins of the nuclear envelope are dispersed throughout the endoplasmic reticulum during mitosis. *J. Cell Biol.* **137,** 1199–1210.
26. Ellenberg, J., Siggia, E. D., Moreira, J. E., Smith, C. L., Presley, J. F., Worman, H. J., and Lippincott-Schwartz, J. (1997). Nuclear membrane dynamics and reassembly in living cells: targeting of an inner nuclear membrane protein in interphase and mitosis. *J. Cell Biol.* **138,** 1193–1206.
27. Macaulay, C., Meier, E., and Forbes, D. J. (1995). Differential mitotic phosphorylation of proteins of the nuclear pore complex. *J. Biol. Chem.* **270,** 254–262.
28. Favreau, C., Worman, H. J., Wozniak, R. W., Frappier, T., and Courvalin, J.-C. (1996). Cell cycle-dependent phosphorylation of nucleoporins and nuclear pore membrane glycoprotein gp210. *Biochemistry* **35,** 8035–8044.
29. Pandey, S., Karande, A. A., Mishra, K., and Parnaik, V. K. (1994). Inhibition of nuclear protein import by a monoclonal antibody against a novel class of nuclear pore proteins. *Exp. Cell Res.* **212,** 243–254.
30. Jagatheesan, G., Thanumalayan, S., Muralikrishna, B., Rangaraj, N., Karande A. A., and Parnaik, V. K. (1999). Colocalization of intranuclear lamin foci with RNA splicing factors. *J. Cell Sci.* **112,** 4651–4661.
31. Fabrizio, P., Laggerbauer, B., Lauber, J., Lane, W. S., and Lührmann, R. (1997). An evolutionarily conserved U5 snRNP-specific protein is a GTP-binding factor closely related to the ribosomal translocase EF-2. *EMBO J.* **16,** 4092–4106.
32. Davis, L. I., and Blobel, G. (1986). Identification and characterization of a nuclear pore complex protein. *Cell* **45,** 699–709.
33. Cordes, V. C., Reidenbach, S., Rackwitz, H. R., and Franke, W. W. (1997). Identification of protein p270/Tpr as a constitutive component of the nuclear pore complex-attached intranuclear filaments. *J. Cell Biol.* **136,** 515–529.
34. Finlay, D. R., and Forbes, D. J. (1990). Reconstitution of biochemically altered nuclear pores: Transport can be eliminated and restored. *Cell* **60,** 17–29.
35. Finlay, D. R., Meier, E., Bradley, P., Horecka, J., and Forbes, D. J. (1991). A complex of nuclear pore proteins required for pore function. *J Cell Biol.* **114,** 169–183.
36. Guan, T., Muller, S., Klier, G., Panté, N., Blevitt, J. M., Haner, M., Paschal, B., Aebi, U., and Gerace, L. (1995). Structural analysis of the p62 complex, an assembly of O-linked glycoproteins that localizes near the central gated channel of the nuclear pore complex. *Mol. Biol. Cell* **6,** 1591–1603.
37. Theodoropoulos, P. A., Polioudaki, H., Koulentaki, M., Kouroumalis, E., and Georgatos, S. D. (1999). PBC68: A nuclear pore

complex protein that associates reversibly with the mitotic spindle. *J. Cell Sci.* **112,** 3049–3059.

38. Nigg, E. A. (1993). Targets of cyclin-dependent protein kinases. *Curr. Opin. Cell Biol.* **5,** 187–193.
39. Burke, B., and Gerace, L. (1986). A cell-free system to study reassembly of the nuclear envelope at the end of mitosis. *Cell* **44,** 639–652.
40. Jordan, M. A., and Wilson, L. (1999). The use and action of drugs in analysing mitosis. *Methods Cell Biol.* **61,** 267–295
41. Maul, G. G. (1977). Nuclear pore complexes: Elimination and reconstruction during mitosis. *J. Cell Biol.* **74,** 492–500.
42. Buendia, B., and Courvalin, J.-C. (1997). Domain specific disassembly and reassembly of nuclear membranes during mitosis. *Exp. Cell Res.* **230,** 133–144.
43. Collas, P., and Courvalin, J.-C. (2000). Sorting nuclear membrane proteins at mitosis. *Trends Cell Biol.* **10,** 5–8.
44. Chaudhary, N., and Courvalin, J.-C. (1993). Stepwise reassembly of the nuclear envelope at the end of mitosis. *J. Cell Biol.* **122,** 295–306.
45. Meier, J., and Georgatos, S. D. (1994). Type B lamins remain associated with the integral nuclear envelope protein p58 during mitosis: Implications for nuclear reassembly. *EMBO J.* **13,** 1888–1898.
46. Macaulay, C., and Forbes, D. J. (1996). Assembly of the nuclear pore, biochemically distinct steps revealed with NEM, GTPS and BAPTA. *J. Cell Biol.* **132,** 5–20.
47. Goldberg, M. W., Wiese, C., Allen, T. D., and Wilson, K. L. (1997). Dimples, pores, star-rings and thin rings on growing nuclear envelopes, evidence for structural intermediates in nuclear pore complex assembly. *J. Cell Sci.* **110,** 409–420.
48. Bodoor, K., Shaikh, S., Salina, D., Raharjo, W. H., Bastos, R., Lohka, M., and Burke, B. (1999). Sequential recruitment of NPC proteins to the nuclear periphery at the end of mitosis. *J. Cell Sci.* **112,** 2253–2264.

Received April 17, 2000
Revised version received August 25, 2000